JOURNAL OF MATERIALS SCIENCE **35** (2000) 1433–1438

Environmental and internal hydrogen embrittlement of a directionally solidified Ni-rich Ni_3Al intermetallics

JIAN-QING SU*,‡, SHU-JUN GAO, ZHUANG-QI HU
Institute of Metal Research, Chinese Academy of Sciences, 72 Wenhua Road, Shenyang 110015, People's Republic of China
E-mail: jqsu@nrim.go.jp

The influence of tensile orientation, test environments and internal hydrogen contents on the room temperature tensile properties of a directionally solidified Ni_3Al alloy was investigated. The specimens parallel to the growth direction exhibited a good ductility and little susceptibility to test environment. The values of elongation in vacuum, air and H_2 are 39.7%, 39.2% and 29.7%, respectively. Also, a transgranular fracture mode was observed in the specimens. However, the specimens perpendicular to the growth direction exhibited lower ductility, much more sensitivity to test environment and intergranular fracture mode. The elongation values in vacuum, air and H_2 are 13.7%, 10.3% and 3.3%, respectively. The results indicate that the cohesive strength of grain boundaries in the alloy is low and they are more susceptible to test environment than are grain interiors. In addition, only a slight embrittlement of the internal hydrogen was found in the specimens parallel to the growth direction.

1. Introduction

Polycrystalline Ni_3Al has long been considered to be brittle [1–3], whereas single crystals of Ni_3Al are known to be ductile [3–5]. For many years the grain boundaries in Ni_3Al were thought to be "intrinsically brittle". Recent studies, however, have shown that environmental embrittlement (an extrinsic factor) is a major cause of the poor ductility of Ni_3Al in air [6–10]. It is widely accepted that the environmental hydrogen embrittlement of polycrystalline Ni_3Al is associated with grain boundary. Hydrogen released from moisture in air or hydrogen gas in environment increases in stress (or stress intensity) at grain boundary [11] or reduces the cohesive strength of grain boundary [12], resulting in an embrittlement.

Hirano recently developed a method to ductilize Ni_3Al by unidirectional solidification using a floating zone technique, which is called FZ-UDS [13–17]. Binary Ni_3Al grown by FZ-UDS, showing a columnar-grained structure, exhibited extensive tensile elongation over 50% [15]. Nishimura *et al*. [18] studied the environmental embrittlement of the Ni_3Al grown by FZ-UDS and indicated that binary Ni_3Al grown by FZ-UDS does not exhibit the moisture-induced environmental embrittlement at room temperature. In addition, the studies by Takasugi *et al*. [19, 20] showed that $Ni_3(Al,Ti)$ single crystal exhibited susceptibility to test environments (e.g. air, hydrogen gas). These results suggest that grain interior is susceptible to environmental embrittlement.

By changing the tensile orientation, this paper studies the mechanical properties of a directionally solidified Ni-rich Ni_3Al alloy with columnar-grained structure and the susceptibility of grain interiors and grain boundaries to test environments. Also the effect of internal hydrogen on the mechanical properties was investigated.

2. Experimental procedure

The purity of the constituent metals, nickel and aluminum, were 99.9 and 99.99 wt%, respectively. A Ni-22.6Al (at%) ingot of $16 \times 66 \times 135$ mm was directionally solidified (DS) by using high rate solidification method from cast ingot of master alloy which was melted in a vacuum induction furnace. The solidification rate was 5×10^{-5} m/s.

Sheet tensile specimens were cut from the as-grown alloy parallel and perpendicular to the growth direction with a spark machine. The dimensions of the gauge section were $1.8 \times 3.0 \times 15$ mm for the specimens parallel to the growth direction and $1.2 \times 2.2 \times 10$ mm for the specimens perpendicular to the growth direction. Optical microscopy and TEM examined the microstructure of the specimens.

To prepare various amounts of internal hydrogen contents in the specimens parallel to the growth direction,

* To whom all correspondence should be addressed.
‡ *Present Address*: Mechanical Properties Division, National Research Institute for Metals, 1-2-1, Sengen, Tsukuba, Ibaraki 305-0047, Japan.

the tensile specimens were annealed in hydrogen gas at a pressure of 0.8 atm for different times (from 10 minutes to 120 minutes) at 750 K, followed by furnace cooling. At the same time, these annealings were performed on specimens that were provided for the chemical analyses of hydrogen contents. Just before annealing, the surface of the specimens was ground on SiC paper to 800 grit and cleaned in methanol. To reduce the loss of hydrogen in specimens, the tensile tests and the chemical analyses were conducted promptly after the heat-treatment in hydrogen gas.

The tensile tests were carried out at room temperature at a strain rate of 1×10^{-3} s^{-1} on a Gleeble 1500 machine equipped with a vacuum chamber. Environment effects were investigated under three conditions: vacuum of about 6.6×10^{-3} Pa, air with relative humidity of 62% and hydrogen gas (H_2) with pressure about 6.7×10^4 Pa. Fracture surface was examined by a scanning electron microscopy and the chemical composition of fracture surface was analyzed by energy dispersive X-ray spectroscopy (EDS).

3. Results

3.1. Microstructure

Fig. 1 shows the optical micrographs of as-grown structure of the ingot. The ingot exhibited a columnar grain structure and the grains were essentially aligned along the solidification direction (Fig. 1a). Optical micrographs at higher magnification reveal a dual-phase structure, where networks of γ-phase are visible (Fig. 1b). The structure is similar to the microstructure observed by Hanada *et al*. [21] in Ni-22.5 Al (at%) single crystal. Fig. lc shows the transverse section microstructure of the DS ingot. The grain boundaries of the columnar grain structure are winding and cut across γ' single-phase area and $\gamma + \gamma'$ dual-phase area simultaneously. Fig. 2a shows electron micrograph of network γ-phase shown in Fig. 1b. Fig. 2b shows a dark field image using a superlattice reflection taken at a network γ-phase in Fig. 2a. The γ-phase contains many cuboidal γ' particles less than 0.1 μm in size.

3.2. Mechanical properties and environmental embrittlement

Table I summarizes the results of room-temperature tensile tests. For each combination of test environment and specimen orientation, three specimens were tested; the values listed in Table I are averages of the three tests. The specimens parallel to the growth direction showed a good ductility and a high ultimate tensile strength (UTS) whether in vacuum or air, and only a limited decrease in elongation and UTS in hydrogen

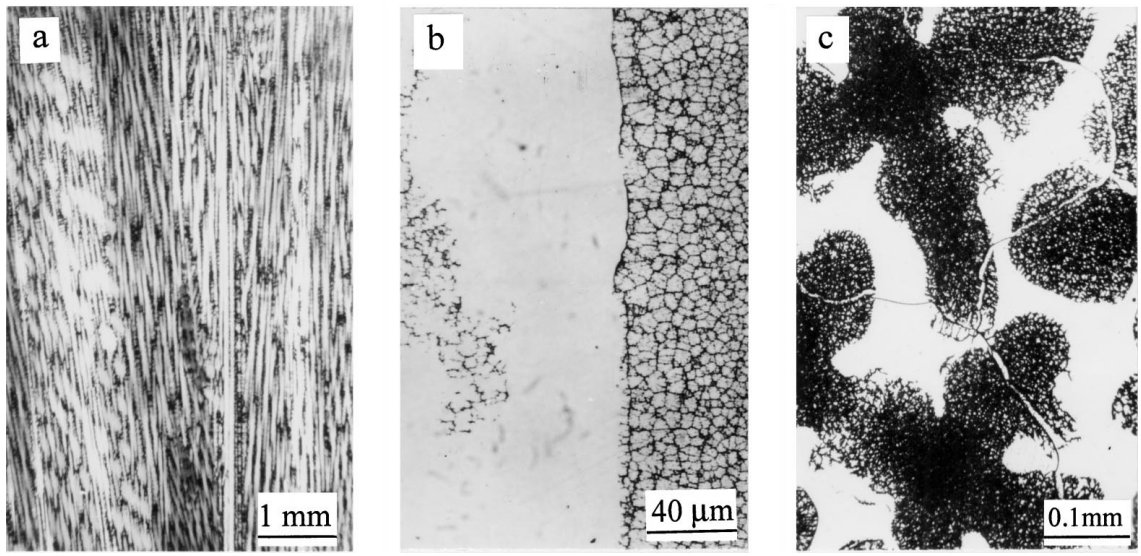

Figure 1 Optical micrographs of Ni_3Al grown by DS. (a) Longitudinal section; (b) higher magnification of (a); (c) transverse section.

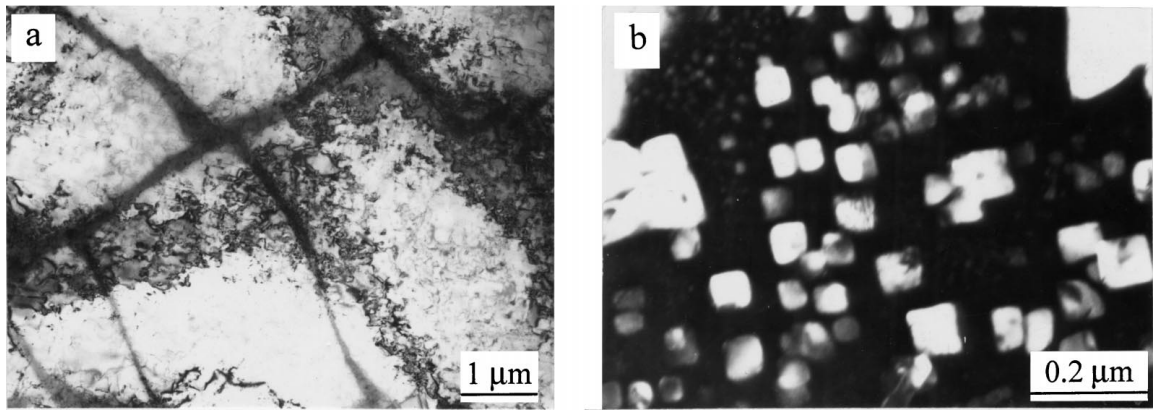

Figure 2 TEM images of network γ-phase containing γ'-phase. (a) Bright field image; (b) dark field image using superlattice reflection of γ'-phase.

TABLE I Effect of test environment and specimen orientation on the room temperature tensile properties of the DS Ni_3Al

Specimen	Test Environment	Strength (MPa) Yield	Strength (MPa) Ultimate	Elongation (%)	I[a] (%)
	Vacuum	274	788	39.7	
//GD[b]	Air	278	782	39.2	1.3
	H_2	277	689	29.7	25.2
	Vacuum	332	493	13.7	
⊥GD	Air	343	437	10.3	24.8
	H_2	337	361	3.3	75.9

[a] I: Embrittlement index.
[b] GD: Growth direction.

gas. Comparing with the specimens parallel to the growth direction, the specimens perpendicular to the growth direction exhibited a lower ductility and UTS, and also a much more sensitivity to test environment. They not only were embrittled severely by hydrogen gas, but also showed a certain susceptibility to air. The yield strength of the two kinds of specimens is not susceptible to test environment.

We describe the extent of environmental embrittlement with the embrittlement index I:

$$I = \frac{(\delta_V - \delta_E)}{\delta_v}$$

Where δ_V and δ_E are the elongations in vacuum and test environments (e.g. air, hydrogen gas), respectively. The embrittlement index of specimens parallel to the growth direction in air and hydrogen gas are 1.3% and 25.2%, respectively, and the values of the specimens perpendicular to the growth direction in air and hydrogen gas are 24.8% and 75.9%, respectively.

3.3. Fracture behavior

Fig. 3 shows the effect of test environments on fractography of the specimens parallel to the growth direction. The fractographys exhibited the dimple-like patterns whenever tested in vacuum or air (Fig. 3a and b), thus revealing very ductile fracture mode. In the specimen tensile-tested in hydrogen gas, a mixture fracture mode of dimple-like and cleavage-like was observed (Fig. 3c); the latter resulted in a decrease of elongation value.

The fracture surface of the specimens perpendicular to the growth direction was not susceptible to test environments and exhibited mainly intergranular separation whenever tested in vacuum, air or hydrogen gas. Fig. 4 shows the fracture surface in air. The fractograph at higher magnification showed that there are some different characteristics at different areas of the fracture surface (Fig. 4b). Some areas showed a clear intergranular fracture and a "ductile-like" pattern was observed in others areas. Elements analysis by EDS showed that the inergranular fracture area is Ni-24.7Al (at.%) and the "ductile-like" area is Ni-16.3Al (at.%). It was considered in this study that the areas showing a clear intergranular brittle fracture are the parts of grain boundary cut across γ' single-phase area, i.e. γ'-γ' grain boundaries, and the areas showing "ductile-like" pattern are the parts of grain boundary cut across $\gamma + \gamma'$ dual-phase area, i.e. $(\gamma + \gamma')$-$(\gamma + \gamma')$ grain boundaries.

3.4. Effect of internal hydrogen

All of the specimens used to charge hydrogen are parallel to the growth direction of the DS alloy. Fig. 5 plots the internal hydrogen content of the specimens as a function of annealing time in hydrogen gas at 750 K. The internal hydrogen content initially increased

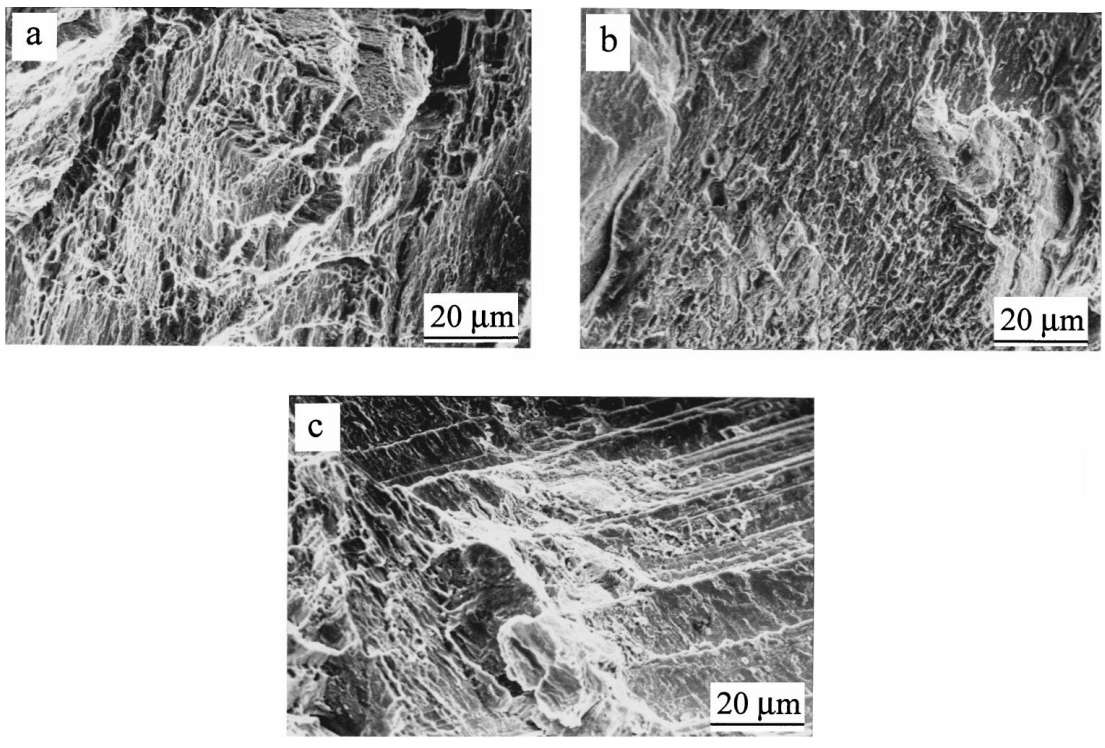

Figure 3 Fracture surface of specimens parallel to the growth direction tested in (a) vacuum, (b) air and (c) hydrogen gas.

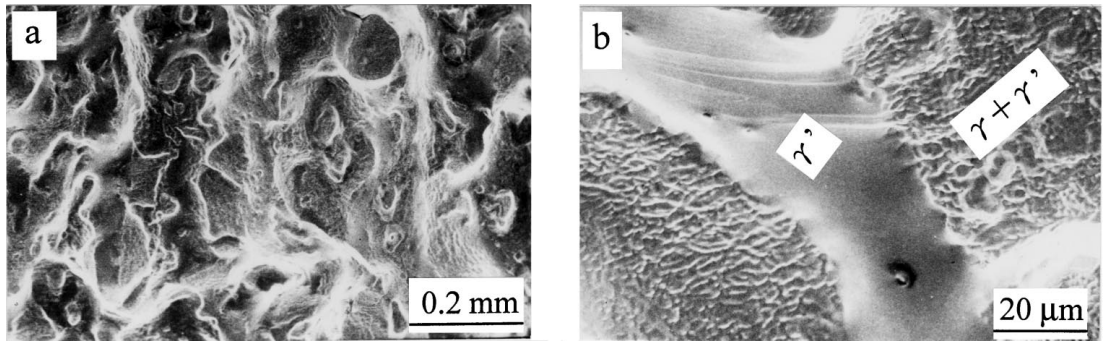

Figure 4 Fracture surface of specimens perpendicular to the growth direction tested in air. (a) Low magnification; (b) higher magnification.

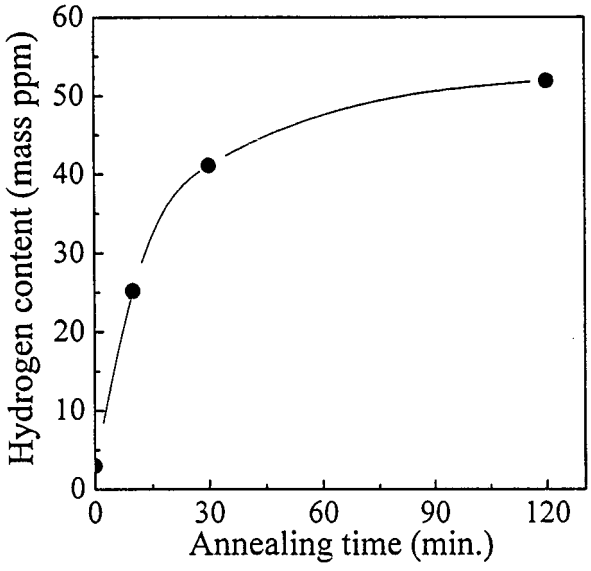

Figure 5 Residual hydrogen contents in specimens as a function of annealing time in hydrogen gas at 750 K.

rapidly and then slowly with increasing annealing time. Tensile specimens of the Ni_3Al containing internal hydrogen with a wide range of contents (i.e. 3.0–51.9 mass ppm) were prepared in this study.

Table II summarizes the tensile results of specimens with various hydrogen contents at room temperature tested in air. The results exhibit that the ductility and ultimate tensile stress (UTS) decreased slightly with increasing the internal hydrogen content. The tensile elongation and UTS changed from 39.2%, 782 MPa at the internal hydrogen content of about 3.0% mass ppm to 34.6%, 722 MPa at the internal hydrogen content of about 51.9 mass ppm, respectively, suggesting that the internal hydrogen caused only a slight hydrogen embrittlement to the alloy. The yield stresses of the specimens were primarily independent of the internal hydrogen contents.

TABLE II Effect of internal hydrogen content on the room temperature tensile properties of the DS Ni_3Al

Charging Time (min.)	Hydrogen (ppm)	Strength (MPa)		Elongation (%)
		Yield	Ultimate	
0	3.0	278	782	39.2
10	25.2	289	776	38.0
30	41.1	286	749	35.8
120	51.9	293	722	34.6

Fig. 6 shows fractography of specimens containing internal hydrogen. The specimens with lower internal hydrogen content exhibited mainly dimple-like patterns (Fig. 6a and b), showing very ductile fracture mode. The specimens with higher internal hydrogen content still exhibited mainly dimple-like patterns, but some cleavage fracture character was observed (Fig. 6c and d), corresponding to some decrease in elongation of the specimens.

4. Discussion

4.1. On the effect of tensile orientation

Hirano [15] studied the tensile deformation behavior at room temperature parallel and perpendicular to the growth direction for the stoichiometric Ni_3Al grown by FZ-UDS. Although the tensile elongation is larger when tensile tested parallel to the growth direction, a good ductility was observed in both directions, and the fracture mode is also independent of the tensile axis. It is a transgranular fracture in both tensile directions, parallel and perpendicular to the growth directions. The results indicate that the grain boundaries grown by FZ-UDS are intrinsically resistant to cracking irrespective of the tensile axis. Nishimura *et al*. [18] suggested that the good ductility of stoichiometic Ni_3Al grown by FZ-UDS must be closely related to its grain boundary character, i.e., low angle and low Σ coincidence boundaries. Our study to the DS material shows that there are great differences in the mechanical properties and fracture mode between samples parallel and perpendicular to the growth direction. The specimens perpendicular to the growth direction exhibited a low ductility and intergranular separation, showing that cohesive strength of grain boundaries of the Ni-rich DS Ni_3Al grown by using high rate solidification method is low. According to the previous work by Hanada *et al*. [22], the gain boundaries in columnar-grained Ni_3Al are mainly high-angle random ones, and they are brittle when tensile-tested in the transverse direction of columnar grains. This is consistent with our test results, indicating that our DS alloys consist of high-angle boundaries. When tensile tested parallel to the growth direction, this type columnar-grained structure minimizes normal stresses across the grain boundary and thus reduces the probability of intergranular fracture,

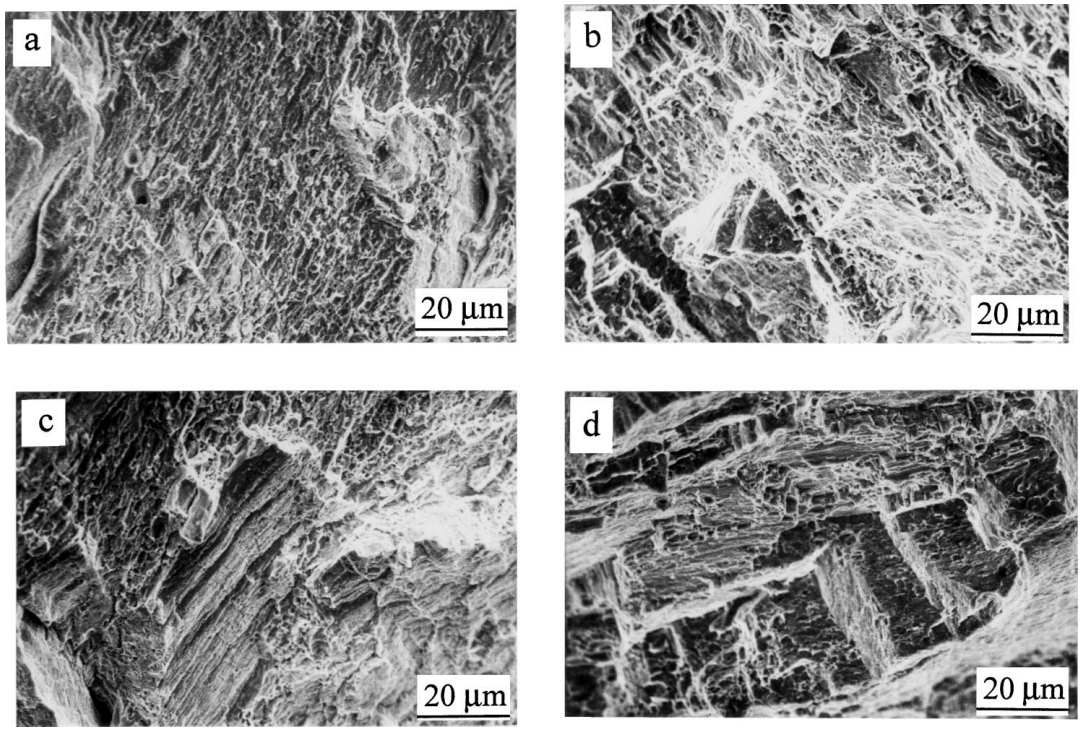

Figure 6 The effect of the internal hydrogen contents on fractography of specimens deformed in air. Note that (a), (b), (c) and (d) show fractography of specimens containing the internal hydrogen contents of 3.0, 25.2, 41.1 and 51.9 massppm, respectively.

even though the boundary is intrinsically weak. Moreover, microcracks formed during early stages of deformation could be arrested by an adjacent grain boundary. This mechanism can act while catastrophic propagation of the crack does not happen. For perpendicular samples horizontal grain boundaries cannot stop temporally crack propagation. Besides, the high stress level (high yield stress) would assist the rapid propagation of the crack.

The present alloy consists of dual-phase, i.e. γ'-phase and γ-phase contained many cuboidal γ' particles less than 0.1 μm in size. The γ-phase containing fine γ'-phase is thought to have strength and toughness [21], as the microstructure of the γ-phase is the same as that in nickel-base superalloy [23]. The superalloys are recognized to be dispersion-strengthened by γ' precipitates dependent on particle size [24]. So the γ-phase also contributed to the good ductility of the specimens parallel to the growth direction. We noted that the specimens perpendicular to the growth direction still exhibit certain ductility even though the elongation value (13.7% in vacuum) is much less than that of specimens parallel to the growth direction (39.7% in vacuum). It is also related to γ-phase. As shown in Fig. 1, Grain boundaries of the alloy cut across γ' single-phase and $\gamma + \gamma'$ dual-phase areas. When a crack nucleated at γ'-γ' grain boundary propagates along the γ'-γ' boundaries, the crack reaches $(\gamma + \gamma')$-$(\gamma + \gamma')$ boundary. The γ-phase can blunt crack propagation.

4.2. Environmental hydrogen embrittlement

Recent work has shown that environmental embrittlement (an extrinsic factor) is a major cause of the poor ductility of polycrystalline Ni_3Al in air [6–9]. The embrittlement mechanism is thought to involve chemical reactions of the following sort [10, 25, 26]:

$$M + H_2O \rightarrow M\text{-}O + H,$$

or

$$M + H_2O \rightarrow M\text{-}OH + H,$$

where M is a reactive element in the intermetallic (e.g. Al in Ni_3Al) which reacts with moisture in air to form the corresponding metal oxide (or hydroxide) and atomic hydrogen, the atomic hydrogen enters into the metal and causes embrittlement. When tested in hydrogen gas, a greater amount of hydrogen atoms can be released from H_2 into the material interior because of catalysis by Ni element and result in a more severe hydrogen embrittlement [27, 28].

Hydrogen atoms coming from environments become distributed in grain interiors or grain boundaries of the alloy, and thus caused grain interior embrittlement or grain boundary embrittlement. When tensile tested parallel to the growth direction, the alloy shows only grain interior embrittlement because normal stress at grain boundaries is minimized. In spite of this the grain boundaries may be weakened by hydrogen segregated there. The present study shows that the grain interior embrittlement of the alloy is not serious. A small amount of hydrogen (tested in air) is not enough to cause embrittlement of grain interior. Even though tensile-tested in hydrogen gas (a greater amount of hydrogen atoms enter into the alloy), the decrease in ductility of the alloy was limited. The fractography also indicates that hydrogen embrittlement within the grains results on areas showing cleavage fracture. However, when tensile tested perpendicularly to the growth direction, the alloy showed a much greater susceptibility to environments.

It was embrittled severely by hydrogen gas, also was embrittled by air, and showed that hydrogen results in intergranular separation. This is due to the hydrogen atoms segregated at grain boundary reducing the cohesive strength of the grain boundaries [12] or increase in stress (or stress intensity) at the grain boundaries [11], resulting in an environmental hydrogen embrittlement. The results show that grain boundaries of the columnar-grained structure DS Ni_3Al alloy are more susceptible to test environment than grain interiors.

4.3. Internal hydrogen embrittlement

The ductility and UTS of the alloy decreased slightly with increasing the internal hydrogen content when tested in air (see Table II). The result suggests that the internal hydrogen only resulted in a slight hydrogen embrittlement to the alloy. It is noted that the hydrogen introduced by cathodic charging can embrittle ductile Ni_3Al (e.g. B-doped Ni_3Al alloy) severely [11, 29]. The different method of charging hydrogen may be an important reason besides the difference of the alloys (containing chemical composition and production technique). In the present study, internal hydrogen contents in the DS Ni_3Al alloy are prepared by annealing in hydrogen gas at 750 K for different times. Hydrogen introduced by this technique is generally homogeneously distributed in specimens without creating the surface damage layer, in contrast to hydrogen introduce by the cathodic charging. The cathodic charging may cause damage to layers on the surface of specimens. Also, segregation of hydrogen at some local area inside the alloys can lead to a more severe embrittlement than homogeneous distribution of hydrogen in the alloy [20].

5. Conclusions

1. The directionally solidified Ni-rich Ni_3Al alloy showed a columnar-grain and a dual-phase ($\gamma + \gamma'$) structure. Longitudinal direction of the columnar grains exhibited good intrinsic ductility and transgranular ductile fracture mode (tested in vacuum). The elongation and UTS decreased greatly when tensile-tested in the transverse direction of columnar grains and the specimens showed intergranular separation, indicating a low cohesive strength of grain boundaries in the alloy.

2. The specimens parallel to the growth direction showed a little sensitivity to test environments. They were not susceptible to air and showed only slight grain interior embrittlement in hydrogen gas. The specimens perpendicular to the growth direction exhibited a severe embrittlement in hydrogen gas. Also, they were embrittled by air. A mechanism of hydrogen results in intergranular separation was shown in the specimens, suggesting that grain boundaries are much more susceptible to test environment than grain interiors.

3. The internal hydrogen became distributed homogeneously, even though a great amount of it (e.g. 51.9 ppm). This hydrogen can only embrittle the specimens parallel to the growth direction slightly. The specimens with a lower internal hydrogen content showed mainly ductile fracture mode, while some of cleavage-like character was observed in the specimens with higher internal hydrogen content.

Acknowledgement

The work was sponsored by the Liaoning Natural Science Foundation, grant no. 971114.

References

1. P. H. THORNTON, R. G. DAVIS and T. L. JOHNSTON, *Metall. Trans*. **1** (1970) 207.
2. E. M. GRALA, in "Mechanical Properties of Intermetallic Compounds," edited by J. H. Westbrook (Wiley, NY, 1960) p. 358.
3. K. AOKI and O. IZUMI, *Trans. Japan Inst. Metals*. **19** (1978) 203.
4. S. M. COPLEY and B. H. KEAR, *Trans. TMS-AIME*. **239** (1967) 977.
5. F. E. HEREDIA and D. P. POPE, *Acta Metall. Mater*. **39** (1991) 2017.
6. C. T. LIU, *Scripta Metall. Mater*. **27** (1992) 25.
7. E. P. GEORGE, C. T. LIU and D. P. POPE, *ibid.* **27** (1992) 365.
8. *Idem*., *ibid.* **28** (1993) 857.
9. *Idem*., *ibid.* **30** (1994) 37.
10. *Idem*., *Acta Mater*. **44** (1996) 1757.
11. A. K. KURUVILLA and N. S. STOLOFF, *Scripta Metall. Mater*. **19** (1985) 83.
12. G. M. BOND, I. M. ROBERTSON and H. K. BIRNBAUM, *Acta Metall. Mater*. **37** (1989) 1407.
13. T. HIRANO, *ibid*. **38** (1990) 2667.
14. T. HIRANO, S. S. CHUNG, Y. MISHIMA and T. SUZUKI, in MRS Symp. Proc. High-Temperature Ordered Intermetallic Alloy IV, edited by L. A. Johnson, D. P. Pope and J. O. Stiegler (MRS, Pittsburgh, PA, 1991) Vol. 213, p. 635.
15. T. HIRANO, *Scripta Metall. Mater*. **25** (1991) 1747.
16. T. TIRANO and T. KAINUMA, *ISIJ Int*. **31** (1991) 1134.
17. T. HIRANO and T. MAWARI, *Scripta Metall. Mater*. **26** (1992) 597.
18. C. NISHIMURA, T. HIRANO and M. AMANO, *ibid.* **29** (1993) 1205.
19. T. TAKASUGI, *Acta Metall. Mater*. **39** (1991) 2157.
20. T. TAKASUGI and S. HANADA, *ibid*. **42** (1994) 3527.
21. S. HANADA, S. WATANABE and O. IZUMI, *J. Mater. Sci*. **21** (1986) 203.
22. S. HANADA, T. OGURA, S. WATANABE, O. IZUMI and T. MASUMOTO, *Acta Metall. Mater*. **34** (1986) 13.
23. P. BEARDMORE, R. G. DAVIES and T. L. HOHNSTON, *Trans. Met. Soc. AIME*. **245** (1969) 1537.
24. W. I. MITCHELL, *Z. Metallkde*. **57** (1966) 586.
25. C. T. LIU, E. H. LEE and C. G. MCKAMEY, *Scripta Metall. Mater*. **23** (1989) 875.
26. N. S. STOLOFF and C. T. LIU, *Intermetallics* **2** (1994) 75.
27. T. TAKASUGI and O. IZUMI, *Acta Metall. Mater*. **34** (1986) 607.
28. X. J. WANG, J. H. ZHU and K. L. JING, *Scripta Metall. Mater*. **26** (1992) 473.
29. HUAXIN LI and T. K. CHAKI, *Acta Metall. Mater*. **41** (1993) 1979.

Received 4 August 1998
and accepted 30 September 1999